

Published in final edited form as:

J Infect Dis. 2008 July 15; 198(2): 258–261. doi:10.1086/589307.

Development of real-time *in vivo* imaging of *Staphylococcus epidermidis* device-related infection in mice: influence of animal immune status

Cuong Vuong^{1,3,*}, Stanislava Kocianova^{†,3}, Yu Jun^{2,††}, Jagath L. Kadurugamuwa^{2,†††}, and Michael Otto^{3,*}

¹Department of Anesthesiology and Department of Molecular Genetics & Microbiology, University of Massachusetts Medical School, Worcester MA, USA

²Xenogen Corp., Alameda, CA, USA

³Rocky Mountain Laboratories, LHBP, NIAID, NIH, Hamilton, MT, USA

Abstract

SUMMARY—We constructed a bioluminescent strain of *Staphylococcus epidermidis* and developed a catheter-related murine infection model for real-time monitoring of biofilm-associated infection in this leading nosocomial pathogen. Additionally, we compared immune-compromised versus immune-competent mice, demonstrating a substantial effect of animal immune status on susceptibility to experimental *S. epidermidis* infection.

Advanced modern detection techniques such as bioluminescence imaging (BLI) utilize a high sensitive optical biophotonic camera and subsequent digital quantification to measure *in vivo* processes. Bioluminescence results from the emission of visible light by metabolically active organisms through luciferase-catalyzed oxidation of the substrate luciferin. The bioactive process requires FMN_{H2}, ATP, and oxygen. Microorganisms can be engineered to produce bioluminescence by insertion of the *lux* genes into the bacterial genome. Thus, BLI permits visualization, quantification, and monitoring of “tagged” microorganism within intact animals (3,4,8,21).

Staphylococcus epidermidis is the leading pathogen in nosocomial infections associated with biofilm formation on medical devices (12,27). Despite the high prevalence of *S. epidermidis* infections in hospitals, not much is known about how *S. epidermidis* biofilms develop in the living host. Almost all animal infection studies require euthanasia at a final time point for the isolation of bacteria from implanted devices and tissues (18). However, samples obtained from these studies represent only a *status quo* of biofilm infection. In contrast, although biofilm-associated factors of *S. epidermidis* (e.g. *ica*, *atlE*, *agr*) have been investigated in several animals (18-20,26), *in vivo* dynamics of *S. epidermidis* biofilm-associated infection have not been monitored.

*Corresponding authors, addresses: Cuong Vuong, Department of Anesthesiology and Department of Molecular Genetics & Microbiology, University of Massachusetts Medical School, 55 Lake Avenue North, S2-717, Worcester, MA-01655, USA, USA. Phone +508-856-8497, Fax +508-856-5911, cuong.vuong@umassmed.edu. Michael Otto, Rocky Mountain Laboratories, National Institute of Allergy and Infectious Diseases, National Institutes of Health, 903 South 4th Street, Hamilton, MT-59840, USA. Phone +406-363-9283, Fax+406-363-9677, motto@niaid.nih.gov.

[†]Department of Anesthesiology, University of Massachusetts Medical School, 55 Lake Avenue North, S2-717, Worcester, MA-01655, USA

^{††}Shanghai Genomics, 647 Song Tao Road, Building 1, Zhangjiang Hi-Tech Park, Pudong New Area, Shanghai 201203, P.R. China

^{†††}Clorox Services Company, 7200 Johnson Drive, Pleasanton, CA-94588, USA

Generation of SE Xen43 and BLI of *S. epidermidis* biofilm in mice

To set up a real-time monitoring model of *S. epidermidis* biofilm-associated infection using BLI, we first genetically engineered a bioluminescent *S. epidermidis* (SE) strain, SE Xen43, by insertion of the *luxABCDE* genes into the genome of the biofilm-positive clinical isolate SE 1457 (13) as reported previously (9,10). In this strain, the *lux* genes had inserted within the intergenic region between the open reading frames SE2196 and SE2197 (31) as determined by inverted PCR sequencing. To ascertain that the bioluminescent strain was phenotypically equal to the parental strain except for light emission, SE Xen43 and SE 1457 were tested *in vitro* for biofilm formation, extracellular polysaccharide production, growth, biochemical profile (API 20 STAPH System and DNase activity), and hemolysis. No significant differences were found between both strains (data not shown). To compare *in vivo* biofilm capacity and virulence of the strains, we used a murine model of subcutaneous device-related infection with exponentially or stationary grown inocula. The two different inocula were selected to evaluate a potential influence of inoculum growth phase on disease progression. The experiment was performed as described previously using Balb/C mice (8 mice, female, 18-25 grams, Charles River, Wilmington, MA, per *S. epidermidis* strain, initial inoculation: 2×10^4 cells/catheter). Mice infected with SE Xen43 were anesthetized daily with gaseous isoflurane for BLI (9,10) with an IVIS 100 imaging system and quantitation using Living Image 2.11 software (Xenogen Corporation, Alameda, CA). Exposure was for a maximum of 5 min. Bioluminescence from predefined regions of interest (ROI) was expressed using a pseudocolor scale with red representing the most intensive and blue the least intensive BLS (9,10). The study protocol was approved by the "Animal Care and Use Committee" of the Rocky Mountain Laboratories.

We monitored progression of biofilm-associated disease caused by SE Xen43 using BLI within intact mice for 7 days (data not shown). Additionally, samples from catheters and surrounding tissues were collected at the final experiment day (day 7) for enumeration of bacterial colony forming units (CFUs) as published (11,25,26). We did not detect significant differences in infectivity between the strains or inocula from different growth phases (Fig. 1A). These results demonstrate that the *luxABCDE* genes insertion in SE Xen43 does not alter the capacity to establish biofilms on plastic polymer material *in vivo* or any other tested *in vitro* characteristics. Hence, SE Xen43 is a suitable strain for *in vivo* research related to *S. epidermidis* infections.

Immune deficiency impacts host susceptibility to biofilm-associated *S. epidermidis* infection

Defects in the host immune system commonly promote microbial infection. Neonatal, immune-compromised or granulocytopenia patients are examples of groups with a particularly high medical risk for *S. epidermidis* infection (17,24,28). Most animal studies of *S. epidermidis* biofilm-associated infection have been performed with immune-competent animals. Therefore, here we investigated how host immune competency impacts *S. epidermidis* biofilm-associated infection. We selected two severe combined immunodeficiency (SCID) mouse strains, Nu/Nu (female, 18-25 gram, Charles River, Wilmington, MA) and CBSCBG-MM (female, 18-25 gram, Taconic Laboratories, Hudson, NY), and compared their susceptibility towards biofilm-associated infection with the immune-competent Balb/C mouse strain. Nu/Nu mice are athymic and T-cell deficient but B-cells and natural killer cells positive (2,15,22,23). CBSCBG-MM mice carry SCID mutation (lack of both T and B lymphocytes), cytotoxic T cells and macrophage defects, and are impaired in natural killer cell function (1,14,16,29). The animal experiment was performed as described above (8 mice per strain) with stationary growth phase cultures of SE Xen43, because (i) we found no significant differences in infection between exponential and stationary growth phase inocula, and (ii) the physiological status of *S. epidermidis* colonizing its natural habitat is presumably more similar to stationary growth phase. Five days before the start of the experiment, administration of antibiotics to the SCID

mice was terminated not to kill *S. epidermidis* cells in the inocula. Biofilms were monitored daily by BLI of SE Xen43 in mice (Fig. 2A). Bioluminescence by SE Xen43 in almost all mice reached a maximum already at 24 h and decreased slowly afterwards (Fig. 2B), most likely due to an activated host immune system. We cannot exclude the possibility that bioluminescence intensity was affected by changes in the metabolic status of the bacteria, which is however a general limitation of BLI in all organisms. A slight increase in bioluminescence was observed in most mice after day 6 indicative of a regeneration of *S. epidermidis* infection or changes in cell metabolism. Notably, CFU determination indicated significantly higher differences in infectivity compared to data obtained from BLI at day 7 (Fig. 1B, Fig. 2B). Importantly, BLI and viable counts (CFUs) data showed that both immune-compromised mice strains were more susceptible towards *S. epidermidis* biofilm infections with Nu/Nu being the most susceptible of all tested strains. Our data clearly support the clinical evidence (5,6,28) that patients with immune deficiency are more susceptible to *S. epidermidis* biofilm-associated infection.

Concluding comments

Our study indicates that SE Xen43 is a suitable tool to study *S. epidermidis* virulence *in vivo* and demonstrates that mice that lack a functional immune system are much more susceptible towards *S. epidermidis* device-related infection compared to healthy mice. The limitation of BLI for *S. epidermidis* is the low intensity in bioluminescence signaling compared to many other bacteria (7,9,30). However, we believe that our results will initiate further investigation on *S. epidermidis* infections, especially to elucidate the specific mechanisms by which *S. epidermidis* evades host defenses *in vivo*.

ACKNOWLEDGEMENT

We would like to thank Ralph Larson, Donald Gardner, and Meghan Kahnle for technical supports with the animal studies.

REFERENCES

1. Andoh M, Zhang G, Russell-Lodrigue KE, Shive HR, Weeks BR, Samuel JE. T cells are essential for bacterial clearance, and gamma interferon, tumor necrosis factor alpha, and B cells are crucial for disease development in *Coxiella burnetii* infection in mice. *Infect Immun* 2007;75:3245–3255. [PubMed: 17438029]
2. Clancy CJ, Nguyen MH, Alandoerffer R, Cheng S, Iczkowski K, Richardson M, Graybill JR. *Cryptococcus neoformans var. grubii* isolates recovered from persons with AIDS demonstrate a wide range of virulence during murine meningoencephalitis that correlates with the expression of certain virulence factors. *Microbiology* 2006;152:2247–2255. [PubMed: 16849791]
3. Contag CH. Molecular imaging using visible light to reveal biological changes in the brain. *Neuroimaging Clin N Am* 2006;16:633–654. [PubMed: 17148024]ix
4. Contag CH, Bachmann MH. Advances in *in vivo* bioluminescence imaging of gene expression. *Annu Rev Biomed Eng* 2002;4:235–260. [PubMed: 12117758]
5. Fleer A, Gerards LJ, Aerts P, Westerdal NA, Senders RC, van Dijk H, Verhoef J. Opsonic defense to *Staphylococcus epidermidis* in the premature neonate. *J Infect Dis* 1985;152:930–937. [PubMed: 4045255]
6. Fleer A, Verhoef J. New aspects of staphylococcal infections: emergence of coagulase-negative staphylococci as pathogens. *Antonie Van Leeuwenhoek* 1984;50:729–744. [PubMed: 6397138]
7. Hardy J, Francis KP, DeBoer M, Chu P, Gibbs K, Contag CH. Extracellular replication of *Listeria monocytogenes* in the murine gall bladder. *Science* 2004;303:851–853. [PubMed: 14764883]
8. Hutchens M, Luker GD. Applications of bioluminescence imaging to the study of infectious diseases. *Cell Microbiol.* 2007

9. Kadurugamuwa JL, Sin L, Albert E, Yu J, Francis K, DeBoer M, Rubin M, Bellinger-Kawahara C, Parr TR Jr, Contag PR. Direct continuous method for monitoring biofilm infection in a mouse model. *Infect Immun* 2003;71:882–890. [PubMed: 12540570]
10. Kadurugamuwa JL, Sin LV, Yu J, Francis KP, Kimura R, Purchio T, Contag PR. Rapid direct method for monitoring antibiotics in a mouse model of bacterial biofilm infection. *Antimicrob Agents Chemother* 2003;47:3130–3137. [PubMed: 14506020]
11. Kocianova S, Vuong C, Yao Y, Voyich JM, Fischer ER, DeLeo FR, Otto M. Key role of poly-gamma-DL-glutamic acid in immune evasion and virulence of *Staphylococcus epidermidis*. *J Clin Invest* 2005;115:688–694. [PubMed: 15696197]
12. Mack D, Rohde H, Harris LG, Davies AP, Horstkotte MA, Knobloch JK. Biofilm formation in medical device-related infection. *Int J Artif Organs* 2006;29:343–359. [PubMed: 16705603]
13. Mack D, Siemssen N, Laufs R. Parallel induction by glucose of adherence and a polysaccharide antigen specific for plastic-adherent *Staphylococcus epidermidis*: evidence for functional relation to intercellular adhesion. *Infect Immun* 1992;60:2048–2057. [PubMed: 1314224]
14. Mahoney E, Reichner J, Bostom LR, Mastrofrancesco B, Henry W, Albina J. Bacterial colonization and the expression of inducible nitric oxide synthase in murine wounds. *Am J Pathol* 2002;161:2143–2152. [PubMed: 12466130]
15. Milon G, Lebastard M, Marchal G. T-dependent production and activation of mononuclear phagocytes during murine BCG infection. *Immunol Lett* 1985;11:189–194. [PubMed: 3910568]
16. Mutwiri GK, Butler DG, Rosendal S, Yager J. Experimental infection of severe combined immunodeficient beige mice with *Mycobacterium paratuberculosis* of bovine origin. *Infect Immun* 1992;60:4074–4079. [PubMed: 1398920]
17. Pfaller MA, Herwaldt LA. Laboratory, clinical, and epidemiological aspects of coagulase-negative staphylococci. *Clin Microbiol Rev* 1988;1:281–299. [PubMed: 3058297]
18. Rupp ME, Fey PD. In vivo models to evaluate adhesion and biofilm formation by *Staphylococcus epidermidis*. *Methods Enzymol* 2001;336:206–215. [PubMed: 11398400]
19. Rupp ME, Ulphani JS, Fey PD, Bartscht K, Mack D. Characterization of the importance of polysaccharide intercellular adhesin/hemagglutinin of *Staphylococcus epidermidis* in the pathogenesis of biomaterial-based infection in a mouse foreign body infection model. *Infect Immun* 1999;67:2627–2632. [PubMed: 10225932]
20. Rupp ME, Ulphani JS, Fey PD, Mack D. Characterization of *Staphylococcus epidermidis* polysaccharide intercellular adhesin/hemagglutinin in the pathogenesis of intravascular catheter-associated infection in a rat model. *Infect Immun* 1999;67:2656–2659. [PubMed: 10225938]
21. Sato A, Klaunberg B, Tolwani R. In vivo bioluminescence imaging. *Comp Med* 2004;54:631–634. [PubMed: 15679260]
22. Serrano-Martinez E, Ferre I, Martinez A, Osoro K, Mateos-Sanz A, Del-Pozo I, Aduriz G, Tamargo C, Hidalgo CO, Ortega-Mora LM. Experimental neosporosis in bulls: parasite detection in semen and blood and specific antibody and interferon-gamma responses. *Theriogenology* 2007;67:1175–1184. [PubMed: 17316779]
23. Sher NA, Chaparas SD, Greenberg LE, Merchant EB, Vickers JH. Response of congenitally athymic (nude) mice to infection with *Mycobacterium bovis* (strain BCG). *J Natl Cancer Inst* 1975;54:1419–1426. [PubMed: 1094126]
24. von Eiff C, Peters G, Heilmann C. Pathogenesis of infections due to coagulase-negative staphylococci. *Lancet Infect Dis* 2002;2:677–685. [PubMed: 12409048]
25. Vuong C, Kocianova S, Voyich JM, Yao Y, Fischer ER, DeLeo FR, Otto M. A crucial role for exopolysaccharide modification in bacterial biofilm formation, immune evasion, and virulence. *J Biol Chem* 2004;279:54881–54886. [PubMed: 15501828]
26. Vuong C, Kocianova S, Yao Y, Carmody AB, Otto M. Increased colonization of indwelling medical devices by quorum-sensing mutants of *Staphylococcus epidermidis* in vivo. *J Infect Dis* 2004;190:1498–1505. [PubMed: 15378444]
27. Vuong C, Otto M. *Staphylococcus epidermidis* infections. *Microbes Infect* 2002;4:481–489. [PubMed: 11932199]

28. Wade JC, Schimpff SC, Newman KA, Wiernik PH. *Staphylococcus epidermidis*: an increasing cause of infection in patients with granulocytopenia. *Ann Intern Med* 1982;97:503–508. [PubMed: 7125409]
29. Wang L, Kamath A, Das H, Li L, Bukowski JF. Antibacterial effect of human V gamma 2V delta 2 T cells in vivo. *J Clin Invest* 2001;108:1349–1357. [PubMed: 11696580]
30. Wiles S, Pickard KM, Peng K, MacDonald TT, Frankel G. In vivo bioluminescence imaging of the murine pathogen *Citrobacter rodentium*. *Infect Immun* 2006;74:5391–5396. [PubMed: 16926434]
31. Zhang YQ, Ren SX, Li HL, Wang YX, Fu G, Yang J, Qin ZQ, Miao YG, Wang WY, Chen RS, Shen Y, Chen Z, Yuan ZH, Zhao GP, Qu D, Danchin A, Wen YM. Genome-based analysis of virulence genes in a non-biofilm-forming *Staphylococcus epidermidis* strain (ATCC 12228). *Mol Microbiol* 2003;49:1577–1593. [PubMed: 12950922]

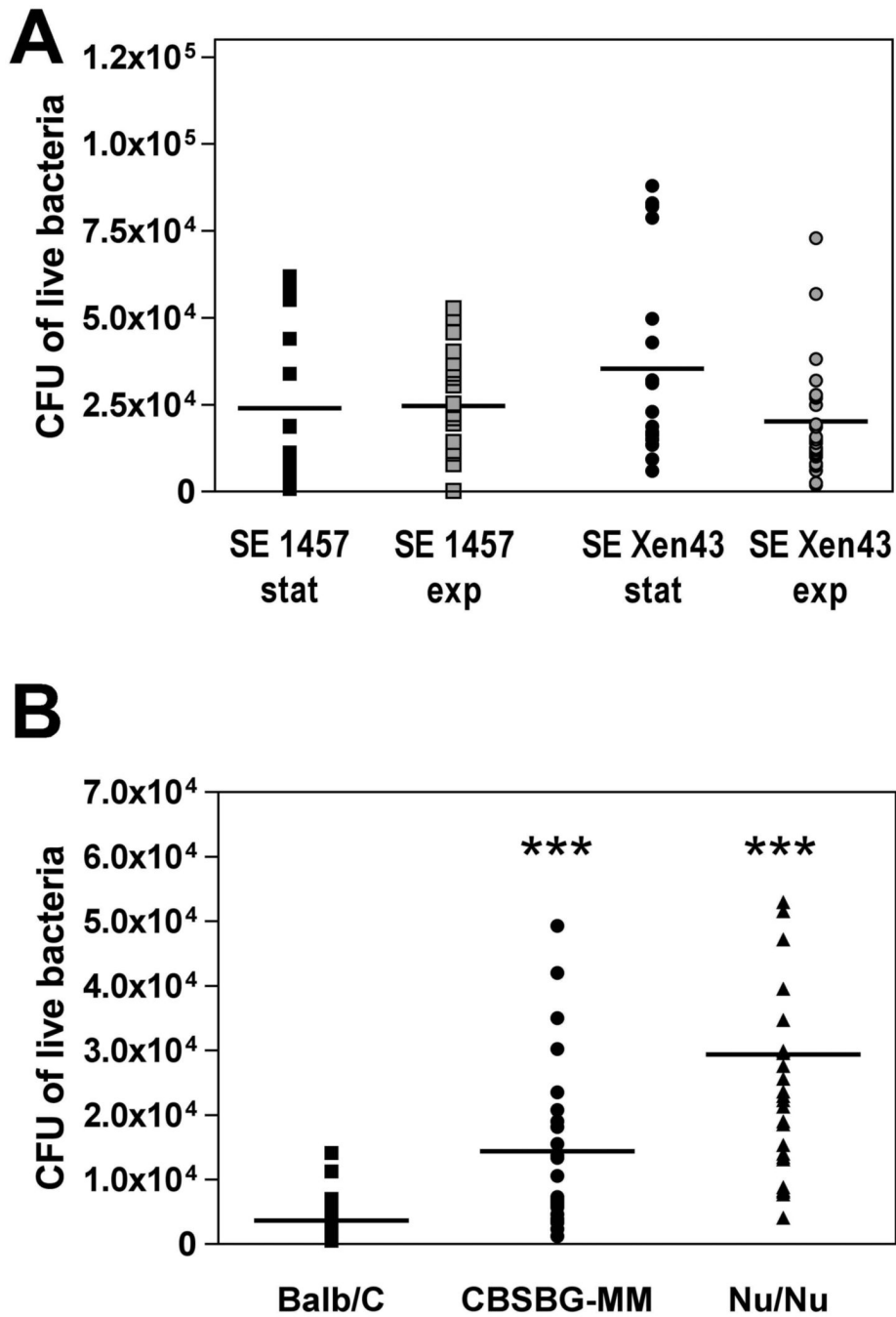


Fig. 1. Mouse biofilm-associated infection model, data from endpoint CFU determination
 (A) Influence of inoculum growth phase and comparison of constructed bioluminescent strain to parental strain. A murine subcutaneous model of device-related infection was utilized to compare infectivity of the parental wild-type strain SE 1457 and its bioluminescent derivative SE Xen43. Exponential and stationary growth phase inocula of both strains were used to determine whether growth phase conditions impact biofilm virulence. After 7 days of infection, mice were killed by isoflurane overdose. Catheters and surrounding tissues were carefully removed from mouse bodies. Bacterial biofilms attached to catheter surfaces were isolated by sonication. Tissues samples were disrupted with a motorized homogenizer. Samples were plated on TSB agar plates, incubated at 37°C for 24 h and bacteria were determined as CFU.

CFU isolated from catheters and surrounding tissues were summarized in the graph. The mean is shown for each group. No statistically significant differences between the groups were detected. **(B)** Comparison of immune-competent with immune-deficient mouse strains. Immune-competent wild-type Balb/C mice, severe combined immunodeficiency mice (SCID) CBSCBG-MM mice, and SCID Nu/Nu mice were tested for their susceptibility towards biofilm-associated infection caused by bioluminescence SE Xen43. CFU counts from catheters and tissue samples were combined. The mean is shown for each group. ***, $p < 0.001$ versus Balb/C group.

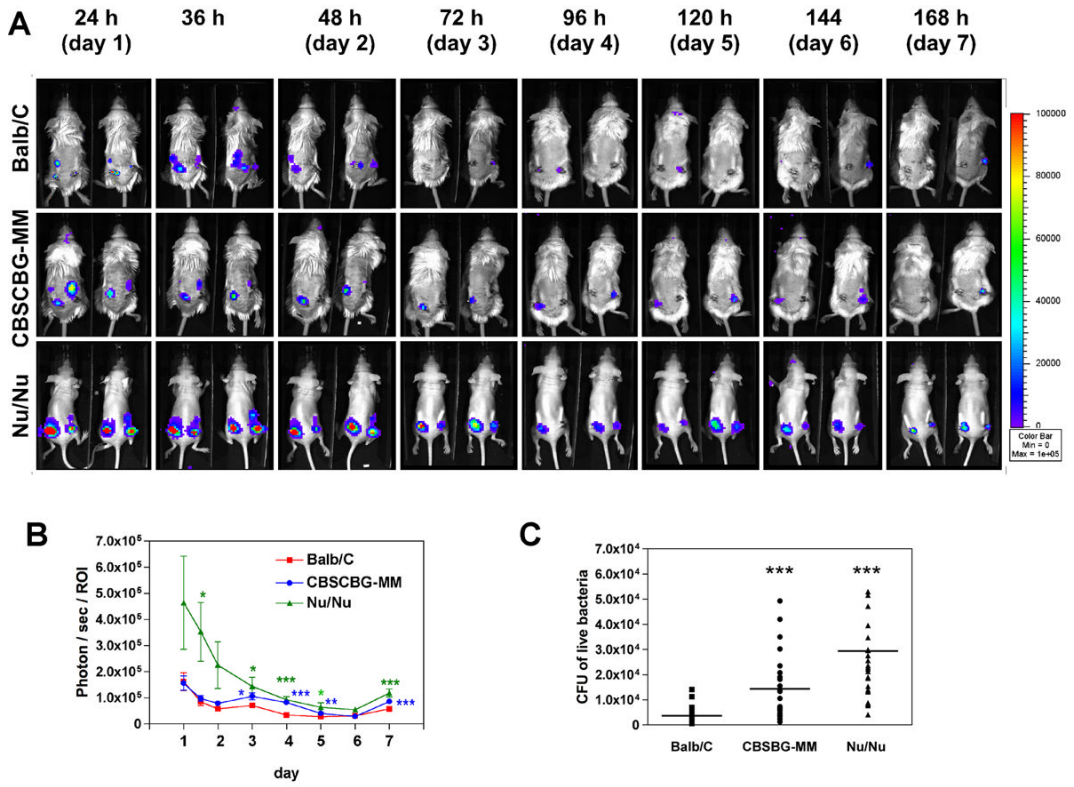


Fig 2. Mouse biofilm-associated infection model, data from real-time monitoring with BLI
(A) Biofilm-associated infection caused by SE Xen43 in intact Balb/C, CBSCBG-MM, and Nu/Nu mice was monitored in real time for 168 h (7 days). Images were taken every 12h for the first 36 h, and every 24 h afterwards. Mice were anesthetized continuously with isoflurane during imaging procedures. Photon/sec/ROI were presented as the cumulative photon counts collected within each measured ROI and quantified with Living Image 2.11 software. **(B)** Quantification of time course dependent bioluminescence of SE Xen43 in Balb/C, CBSCBG-MM, and Nu/Nu mice.